HHS Public Access

Author manuscript

Am J Ophthalmol. Author manuscript; available in PMC 2021 January 01.

Published in final edited form as:

Am J Ophthalmol. 2020 January ; 209: 18–26. doi:10.1016/j.ajo.2019.09.017.

Correlations between Different Choriocapillaris Flow Deficit Parameters in Normal Eyes using Swept Source OCT Angiography

Yingying Shi[1], **Qinqin Zhang**[2], **Fang Zheng**[1], **Jonathan F. Russell**[1], **Elie H. Motulsky**[1], **James T. Banta**[1], **Zhongdi Chu**[2], **Hao Zhou**[2], **Nimesh A. Patel**[1], **Luis de Sisternes**[3], **Mary K. Durbin**[3], **William Feuer**[1], **Giovanni Gregori**[1], **Ruikang K. Wang**[2], **Philip J. Rosenfeld**[1]

[1]Department of Ophthalmology, Bascom Palmer Eye Institute, University of Miami Miller School of Medicine, Miami, Florida, USA

[2]Department of Bioengineering, University of Washington, Seattle, Washington, USA

[3]Research and Development, Carl Zeiss Meditec, Inc., Dublin, CA, USA

Abstract

Purpose: Choriocapillaris (CC) imaging of normal eyes with swept-source optical coherence tomography SS-OCTA was performed, and the percentage of CC flow deficits (FD%) and the average area of CC flow deficits (FDa) were compared within given macular regions.

Design: A prospective, cross-sectional study.

Methods: Subjects with normal eyes ranging in age from their 20s through their 80s were imaged with SS-OCTA (PLEX Elite 9000, Carl Zeiss Meditec, Dublin, CA) using both 3×3 mm and 6×6 mm macular scan patterns. The CC images were generated using a previously published and validated algorithm. In both 3×3 mm and 6×6 mm scans, the CC FD% and FDa were measured in circular regions centered on the fovea with diameters as 1mm and 2.5 mm (C_1 and $C_{2.5}$). In 6×6 mm scans, the FD% and FDa were measured within an additional circular region with diameter as 5 mm (C_5). The correlations between FD% and FDa from each region were analyzed with Pearson's correlation coefficients.

Results: A total of 164 eyes were analyzed. There was excellent correlation between CC FDa and FD% measurements from each region. In the 3×3 mm scans, the correlations in the C_1 and $C_{2.5}$ regions were 0.83 and 0.90, respectively. In the 6×6 mm scans, the correlations in C_1, $C_{2.5}$, and C_5 regions were 0.90, 0.89, and 0.89, respectively.

Conclusions: When measuring CC FDs, we found excellent correlations between FDa and FD% in regions from 3×3 mm and 6×6 mm scans. Further studies are needed to determine if one parameter is more useful when studying diseased eyes.

Corresponding Author: Philip J. Rosenfeld MD, PhD, Bascom Palmer Eye Institute, 900 NW 17th street, Miami, FL, 33136, Voice: 305-326-6148, Fax: 305-326-6538, prosenfeld@miami.edu.

INTRODUCTION

The choriocapillaris (CC) is a single capillary layer located under Bruch's membrane (BM) and provides metabolic support for the outer retina, retinal pigment epithelium (RPE), and choroidal stroma.[1, 2] In a histopathological study using autopsy eyes, Ramrattan et al. found the CC vascular density decreased with age in normal eyes.[3] With the advent of optical coherence tomography angiography (OCTA), CC can be visualized and quantified *in vivo*.[4–8] Consistent with the histological findings, OCTA studies have confirmed an age-dependent CC flow impairments with the greatest impairment in the central macula.[4, 9, 10] In addition, CC flow impairments evaluated using OCTA has been reported in eyes with diseases such as age-related macular degeneration (AMD), diabetic retinopathy, central serous chorioretinopathy, retinitis pigmentosa, idiopathic epiretinal membrane, Vogt-Koyanagi-Harada disease, and Alport syndrome.[5, 11–19] However, the extent of CC flow impairments reported from different studies have been difficult to compare because different instruments and algorithms have been used to generate and analyze the CC *en face* flow images and because the capillaries of the CC are beyond the resolution of commercial OCTA instruments so investigators lack the ground truth evidence that they are truly imaging the CC *in vivo* based on OCTA images.[8–12, 14–17, 20–25]

Different terms have been used to evaluate CC flow and flow impairments such as CC vessel flow density (VFD), vessel density (VD), vessel diameter index (VDI), perfusion density (PD), vessel length density (VLD), flow voids (FVs), grey value (GV), signal voids, percent choriocapillaris area of nonperfusion (PCAN),[8, 9, 20–26] but we prefer to use the term flow deficits (FDs), since these areas represent regions of undetectable CC flow when using a particular instrument and algorithm rather than the absolute absence of physiological CC flow, since flow might be detectable under different circumstances.[5, 7]

We recently reported the age-dependent CC FD percentage (FD%) changes within the macula using SS-OCTA imaging.[4] Overall, the CC FD% was found to be increased with age, but the greatest increase was found in the 1mm circle (C_1) region centered on the fovea.[4] Later, we performed a study to explore the relationship between the annual enlargement rates (ERs) of geographic atrophy (GA) in late non-exudative AMD and the CC FDs around the GA.[27] We found a good linear correlation between ERs and the CC FD%, but there was an even stronger linear correlation between ERs and the average area of individual CC flow deficits (FDa). Even though both CC FD% and FDa measurements were highly correlated with each other in eyes with GA, they represent different parameters that are not mutually exclusive. Based on processed CC binary images, FD% is defined as the number of pixels that represent areas with an undetected flow signal divided by the total pixels in a giving area. CC FDa is defined instead as the average area of the pixels representing flow deficits in a giving area. Our previous findings were that both FD% and FDa were correlated with GA growth and FDa had a stronger correlation with GA growth. Since an enlarging FD area may have a greater detrimental effect on the overlying RPE and photoreceptors than multiple smaller FDs and have a greater influence on the growth of GA, especially at the margins of GA, we wanted to explore if these enlarging FD areas also had a stronger correlation with aging when compared with FD% in our normative database. After all, if we want to compare the CC FDs in diseased eyes with age-matched normal control eyes to determine if any

disease-specific differences exist, then we need to know how all the different parameters used to measure CC FDs behave in normal eyes. This current study reports on the comparison between these two CC FD parameters, FD% and FDa, in normal eyes over seven decades of life.

METHODS

This prospective study was approved by the institutional review board of University of Miami Miller School of Medicine. Informed consent was obtained from each enrolled subject. The study was performed in accordance with the tenets of the Declaration of Helsinki and complied with Health Insurance Portability and Accountability Act of 1996.

Subjects with normal eyes from their 20s through their 80s were enrolled in this study at the Bascom Palmer Eye Institute from November 2016 through February 2018 as described previously.[4] Both eyes from each subject were scanned using SS-OCTA (PLEX® Elite 9000, Carl Zeiss Meditec, Dublin, CA), and the right eye was the default eye unless the image quality was poor due to gross eye movements or weak signal strength (less than seven) as defined by the manufacturer. Subjects with uncontrolled hypertension and diabetes mellitus even without any evidence of diabetic retinopathy were excluded from the study. Eyes with any history of ocular disease, retinal or choroidal pathology, a refractive error ≥ −6.0 diopters or axial length (AL) ≥ 26.00 mm were excluded. AL was measured on each eye using noncontact biometry instrument (IOL master, Carl Zeiss Meditec).

SS-OCTA images were obtained using the instrument with a scanning rate of 100,000 A-scans per second, a central wavelength of 1060 nm, and a full width at half-maximum axial resolution of ~5μm in tissue. Both 3×3 mm and 6×6 mm scan patterns centered on the fovea were performed on each eye. FastTrack™ motion correction software was used during image acquisition. Each 3×3 mm scan consisted of 300 A-scans per B-scan with four repeats at each position before moving to the next sequential B scan location, which results in a homogenous sampling grid with an A-scan and B-scan separation of 10 μm. Each 6×6 mm scan consisted of 500 A-scans per B-scan. Two repeated B-scans were performed at each position resulting in a homogenous sampling grid with a separation of 12 μm.

Flow images were generated by applying the OMAG^{c} algorithm and first normalized to reach a signal strength of nine before further analysis.[28] We recently investigated the CC in normal eyes over a range of ages using swept source OCTA (SS-OCTA). CC flow was detected using the complex optical microangiography (OMAG^{c}) algorithm as previously described.[6, 28–31] The CC *en face* flow images were generated using a semi-automatic segmentation method using a 20 μm thick slab that followed the contour of BM and was about 10 μm under BM,[28, 29, 31–33] A compensation strategy using the corresponding CC *en face* structural images was adopted to adjust for any signal loss in the CC *en face* flow images due to the overlying anatomy.[28, 33] Retinal vessel projection artifacts were removed and a global thresholding method (standard deviations of the CC from 20 young subjects) was applied to the CC *en face* flow images to generate the CC FD binary maps.[33, 34] The final step was to remove the isolated segmented regions with an equivalent diameter smaller than 24 μm from the CC FD binary maps, as they were presumed to be smaller than the

estimated ICD and thus most likely represent noise.[6, 35] CC FDa was measured based on the final processed CC binary maps. While CC FD% was defined as the number of pixels representing FDs divided by the total pixels within a given region, the CC FDa was defined as the total area of all the pixels which represent CC FDs divided by the number of FDs within a given region (Figure 1).[27] For 3×3 mm scans pattern, we analyzed CC FDa in circles centered on the fovea with diameters as 1 mm (C_1) and 2.5 mm ($C_{2.5}$), and we analyzed an additional circle region with diameter as 5 mm (C_5) in the 6×6 mm scan pattern as described in our previous study.[4]

The mean and normal range of CC FDa from each region and each decade was calculated and analyzed using a linear regression model. We then compared the CC FDa measurements with the CC FD% measurements from the same regions and age groups, which were reported in our previous study.[4] The correlations between the CC FDa and FD% measurements were analyzed using Pearson's correlation coefficients. In addition, the CC FDa measurements from the C_1 and $C_{2.5}$ regions in the 3×3 mm and 6×6 mm scans were compared and correlated. Statistical analyses were performed using the IBM Statistical Package for the Social Sciences (SPSS) software version 24 (IBM Corporation, Armonk, NY) with a p-value of <0.05 considered to be statistically significant.

RESULTS

A total of 164 normal eyes from 164 participants were enrolled in this study with a mean AL of 23.00 mm (SD = 1.0 mm). The mean age of all the subjects was 56 years (SD = 19 years, range [19, 88]) and women comprised 56% of all the population.

There were no correlations between CC FDa measurements and AL in normal eyes (all $|r| < 0.15$, all $p > 0.05$). The CC FDa measurements from all the regions were increased with age in both the 3×3 mm and 6×6 mm scans. The mean of the CC FDa measurements, their standard deviations (SDs), and their ranges in each decade of life and within each region from the 3×3 mm scans are shown in Table 1. The age-related CC FDa increases were greater in the C_1 region compared with the $C_{2.5}$ region from 3×3 mm scans. Table 2 shows the FDa measurements for the 6×6 mm scans. Consistent with the results from the 3×3 mm scans, the age-related CC FDa measurements were greater in C_1 region compared with the $C_{2.5}$ and C_5 regions from the 6×6 mm scans. For each region in each scan pattern, linear regression models using FDa with respect to age were fitted, and highly significant relationships for each parameter were found (all $P < 0.001$).

Figure 2 shows the correlations of CC FDa and FD% in the C_1 (A) and $C_{2.5}$ (B) regions from the 3×3 mm scans. The CC FDa and FD% from the C_1 and $C_{2.5}$ regions were highly correlated with each other, and the correlations were $r = 0.83$ and $r = 0.90$, respectively. Figure 3 shows the correlations of CC FDa and FD% in C_1 (A), $C_{2.5}$ (B) and C_5 (C) regions from the 6×6 mm scans. The CC FDa and FD% from the C_1, $C_{2.5}$, and C_5 regions were highly correlated with each other, and the correlations were $r = 0.90$, $r = 0.89$, $r = 0.89$, respectively. In C_1 regions, there was evidence of greater non-linearity resulting in stronger non-parametric Spearman correlations ($rho_{3\times3} = 0.95$ and $rho_{6\times6} = 0.94$) than the more linear plots. Figure 4 shows correlations between the CC FDa measurements in the C_1 and

$C_{2.5}$ regions from the 3×3 mm scans and the C_1 and $C_{2.5}$ regions from the 6×6 mm scans, and these correlations were r = 0.72 and r = 0.56, respectively.

DISCUSSION

The CC FDa measurements were highly correlated with the CC FD% measurements from 164 normal eyes over seven decades of life. In our previous work, we found that CC FD% increased with age, especially in the central 1 mm area under fovea. Similar age-related changes were found when using CC FDa to quantify CC. In a given eye, CC FDa measured the average size of the CC flow deficits contained in a specified region. Therefore, FD% is proportional to FDa times the number of flow deficits in the region, and these factors may vary depending on the different regions being considered. Our previous study correlating baseline CC FDs measurements with annual ERs of GA showed that the CC FDa measurements had better correlations with ERs of GA compared with CC FD%, which suggested that the average size of the CC FDs may contribute more to GA formation and GA enlargement than the overall percentage of FDs.[27] Future studies will explore the relationship between FDs size and the formation and growth of GA, but this relationship seems intuitively more obvious than FD% given the suspicion that GA may form and progress due to the progressive loss of CC perfusion and the size of this perfusion deficit may correlate with localized ischemia and the subsequent loss of the retinal pigment epithelium. Moreover, future studies also need to investigate whether CC flow impairment correlates with other pathologies in AMD, such as drusen and macular neovascularization (MNV), and whether differences exist between CC FD% and FDa in these eyes.

Combined with our previous study, we now have provided normative data to understand how CC FDa and FD% change in different regions of the macula with normal aging.[4] An increase in CC flow impairment was observed in the central macula during the normal aging process without the development of obvious pathology. This leads to the hypothesis that such an increase in FDs may contribute to the onset and severity of disease in individuals who are at risk for pathologies associated with aging, such as AMD. Moving forward, we hope to leverage this information to better understand the role of CC flow impairments plays in different pathologies combined with genetics and the overall health status of the patients. This research represents a work in progress, and our ability to evaluate CC FDs and flow velocity within the CC will improve as SS-OCTA technology evolves.[35–37]

Given the intrinsic difficulties in imaging and quantifying CC features, and the fact that a number of studies have recently appeared in the literature using different instruments, algorithms, and terminologies that may yield disparate conclusions, we believe it is important at this time to reflect on the best strategies for measuring CC flow impairment. We recommend that whatever instrument is used, the researchers should only employ an algorithm that has been validated. The validation of CC algorithm should focus on both qualitative CC visualization and quantitative CC analysis. As a first step to provide qualitatively CC *en face* flow image, a segmentation strategy should be adopted that is parallel and under BM rather than a segmentation strategy that follows the RPE, especially in pathological eyes with elevations of the RPE such as drusen in which the light scattering properties of the RPE and the signal attenuation of the drusen may cause variability in the

appearance of the CC.[33] To be consistent with histological findings, the generated Cc *en face* images should be able to show the lobular pattern of the CC, especially in the peripheral regions, since the CC vessels cannot be visualized in the central macula since these capillaris are beyond the resolution of current commercial OCTA instruments.[3, 33] Furthermore, the CC flow appearance should be consistent in the same region when using different scan patterns and should also be consistent between averaged scans when using the same scan pattern.[33, 38] As the first step for CC quantitative analysis, proper terminologies to describe FDs should be used, and there are certain parameters that should be avoided. Vessel parameters such as PD, VLD and VDI have been used to quantify CC changes with age, [8, 9, 20, 21] but these measurements cannot be meaningfully computed from CC images due to the limitations of current OCTA technologies, since the CC vessels within the macula are typically below the lateral resolution of the instruments. Similarly, parameters like GV,[8] defined as the mean, greyscale intensity value of all pixels in the region of interest are problematic since the greyscale intensity produced by OCTA technologies is influenced by a number of factors such as flow velocity, wavelength, inter-scan times, projection artifacts from the retina, focusing, and anatomic alterations overlying the cC[5, 7, 39–41] Very small FDs, with diameters below the transverse resolution of the particular instrument and/or scanning pattern should be viewed with suspicion and removed from the analyses. Previously, the term of FVs, which was used to describe an area without detectable flow, is a misnomer.[20] Just because the flow was not detectable does not mean it represents a true flow void. Moreover, CC analysis using different OCTA instruments should consider the limitation of SD-OCTA instrument for CC visualization compared to SS-OCTA.[20, 42] SD-OCTA operates at 840 nm wavelength, which is heavily scattered by the RPE complex, and thus affects the ability to visualize CC. However, SS-OCTA operates at a wavelength of about 1060 nm, which results in less scattering by the RPE and less sensitivity roll-off for choroidal imaging compared with SD-OCT imaging. Moreover, SS-OCTA instruments have faster scanning rates and denser scan patterns, which results in better CC images compared with SD-OCTA instruments.

Sacconi et al. investigated CC in 72 normal eyes using SS-OCTA.[9] Although they found that CC perfusion density decreased with aging and this decrease was greater in the foveal region compared to parafoveal region, the repeatability and reproducibility of their algorithm was not analyzed. While they reported the CC perfusion density was significantly decreased in the foveal region compared to parafoveal regions in subjects, they showed differences in significance between their 3×3 mm and 6×6 mm scans, and they found inconsistent changes when comparing different groups as they age, particularly those in their 30s and 50s compared with other decades of life.[9] We did not observe these internal inconsistencies, and their internal discrepancies, as well as their differences compared with our results, most likely arise from their use of an algorithm that was not validated. Using the same instrument, we found that CC flow impairments increase with age in normal eyes especially within the C_1 region and the results were consistent when using different scan patterns (3×3 mm and 6×6 mm scans) and different parameters (FD% and FDa), and these results support the strengths of our approach. The usefulness of a validated algorithm become even more important when analyzing eyes with different pathologies.

In our current study, the CC FDa measured in the 3×3 mm scans were correlated with CC FDa from the 6×6 mm scans, but the value of CC FDa from the 3×3 mm scans tended to be smaller than the values from 6×6 mm scans. This was primarily due to the different scanning parameters of different patterns. The 3×3 mm scans have a spacing distance of 10 μm between A-scans and B-scans while the 6×6 mm scans have a spacing of 12 μm. In addition, the B-scans are repeated four times in the 3×3 mm scans and repeated twice in the 6×6 mm scans. Thus, the 6×6 mm scan has less averaging and greater separation, which we hypothesize results in greater average FD size measurements. As scanning speeds increase and denser scan patterns are achieved, the measurement differences between different scan patterns should become less apparent.

One of the limitations in our current study is that we did not stratify patients based on their systemic diseases other than excluding patients with diabetes and uncontrolled hypertension. Future studies are needed to investigate how cardiovascular disease, hypertension, and other systemic disease affect the CC perfusion over time. Future studies should explore how the duration of systemic diseases, the number and duration of medications, and the types of interventional procedures affects CC flow impairment. Another limitation is that our compensation strategy, although superior to other strategies for processing CC images, is not always successful in completely restoring the OCT signal in areas where overlying retinal structures significantly attenuate the light source. While it is not possible to restore a signal in some areas where the signal is completely attenuated, we are now developing and testing other compensation and thresholding strategies that should improve our ability to provide better CC images. These approaches could be extremely useful in studying a wide range of eye diseases, especially AMD in eyes with drusen, neovascularization, or GA. Our algorithm provides CC images showing a morphology similar to histological findings. In addition, our previous work demonstrated qualitative and quantitative similarities between different scan patterns, repeated scans, and different studies[4, 33, 34] Nevertheless, improvements in OCTA technology will help us further understand the CC in vivo and approach the results given by histology or OCT with adaptive optics.[35]

In summary, we used SS-OCTA to investigate CC FDa changes with age in normal eyes and our results were consistent with previously reported age-related CC FD% changes. While both parameters are strongly correlated with each other, CC FDa and FD% represent different features of CC flow impairment. Studies are ongoing to investigate how these two parameters correlate with the onset, severity, and progression of various retinal and macular diseases.

ACKNOWLEDGMENTS/DISCLOSURES:

a. **Funding/Support:** Research supported by grants from Carl Zeiss Meditec, Inc. (Dublin, CA), the National Eye Institute (R01EY024158, R01EY028753), the Salah Foundation, an unrestricted grant from the Research to Prevent Blindness, Inc., New York, NY, and the National Eye Institute Center Core Grant (P30EY014801) to the Department of Ophthalmology, University of Miami Miller School of Medicine. The funding organization had no role in the design or conduct of this research.

b. **Financial Disclosures:** Dr. Gregori, Dr. Wang and Dr. Rosenfeld received research support from Carl Zeiss Meditec, Inc. Dr. Gregori and the University of Miami co-own a patent that is licensed to Carl Zeiss Meditec, Inc. Dr. Rosenfeld is a consultant for Apellis, Boehringer-Ingelheim, Carl Zeiss Meditec, Chengdu Kanghong Biotech, Healios K.K, Hemera Biosciences, F. Hoffmann-La Roche Ltd., Isarna Pharmaceuticals, Lin Bioscience, NGM Biopharmaceuticals, Ocunexus Therapeutics,

Ocudyne, and Unity Biotechnology. Dr. Rosenfeld has equity interest in Apellis, Verana Health, and Ocudyne. Dr. Wang discloses intellectual property owned by the Oregon Health and Science University and the University of Washington related to OCT angiography, and licensed to commercial entities, which are related to the technology and analysis methods described in parts of this manuscript. Dr. Wang also receives research support from Tasso Inc. He is a consultant to Insight Photonic Solutions, and Kowa. Drs. de Sisternes and Durbin are employed by Carl Zeiss Meditec, Inc. Drs. Shi, Zhang, Zheng, Russell, Motulsky, Banta, Zhou, and Patel have no disclosures. Miss. Chu and Mr. Feuer have no disclosures. All authors attest that they meet the current ICMJE criteria for authorship.

REFERENCES

1. Olver JM. Functional anatomy of the choroidal circulation: methyl methacrylate casting of human choroid. Eye (Lond) 1990;4 (Pt 2):262–72. [PubMed: 2379644]
2. Fryczkowski AW. Anatomical and functional choroidal lobuli. Int Ophthalmol 1994;18:131–41. [PubMed: 7852018]
3. Ramrattan RS, van der Schaft TL, Mooy CM, de Bruijn WC, Mulder PG, de Jong PT. Morphometric analysis of Bruch's membrane, the choriocapillaris, and the choroid in aging. Invest Ophthalmol Vis Sci 1994;35:2857–64. [PubMed: 8188481]
4. Zheng F, Zhang Q, Shi Y, et al. Age-Dependent Changes in the Macular Choriocapillaris of Normal Eyes Imaged with Swept-Source OCT Angiography. Am J Ophthalmol 2019;200:110–122. [PubMed: 30639367]
5. Choi W, Moult EM, Waheed NK, et al. Ultrahigh-Speed, Swept-Source Optical Coherence Tomography Angiography in Nonexudative Age-Related Macular Degeneration with Geographic Atrophy. Ophthalmology 2015;122:2532–44. [PubMed: 26481819]
6. Zhang Q, Shi Y, Zhou H, et al. Accurate estimation of choriocapillaris flow deficits beyond normal intercapillary spacing with swept source OCT angiography. Quant Imaging Med Surg 2018;8:658–666. [PubMed: 30211033]
7. Moult EM, Waheed NK, Novais EA, et al. Swept-Source Optical Coherence Tomography Angiography Reveals Choriocapillaris Alterations in Eyes with Nascent Geographic Atrophy and Drusen-Associated Geographic Atrophy. Retina 2016;36 Suppl 1:S2–S11. [PubMed: 28005659]
8. Al-Sheikh M, Falavarjani KG, Pfau M, Uji A, Le PP, Sadda SR. Quantitative Features of the Choriocapillaris in Healthy Individuals Using Swept-Source Optical Coherence Tomography Angiography. Ophthalmic Surg Lasers Imaging Retina 2017;48:623–631. [PubMed: 28810037]
9. Sacconi R, Borrelli E, Corbelli E, et al. Quantitative changes in the ageing choriocapillaris as measured by swept source optical coherence tomography angiography. Br J Ophthalmol 2019;103:1320–1326. [PubMed: 30361273]
10. Nassisi M, Baghdasaryan E, Tepelus T, Asanad S, Borrelli E, Sadda SR. Topographic distribution of choriocapillaris flow deficits in healthy eyes. PLoS One 2018;13:e0207638. [PubMed: 30440050]
11. Chatziralli I, Theodossiadis G, Panagiotidis D, Pousoulidi P, Theodossiadis P. Choriocapillaris' alterations in the presence of reticular pseudodrusen compared to drusen: study based on OCTA findings. Int Ophthalmol 2018;38:1887–1893. [PubMed: 28779271]
12. Alten F, Heiduschka P, Clemens CR, Eter N. Exploring choriocapillaris under reticular pseudodrusen using OCT-Angiography. Graefes Arch Clin Exp Ophthalmol 2016;254:2165–2173. [PubMed: 27193430]
13. Borrelli E, Uji A, Sarraf D, Sadda SR. Alterations in the Choriocapillaris in Intermediate Age-Related Macular Degeneration. Invest Ophthalmol Vis Sci 2017;58:4792–4798. [PubMed: 28973325]
14. Corbelli E, Sacconi R, Rabiolo A, et al. Optical Coherence Tomography Angiography in the Evaluation of Geographic Atrophy Area Extension. Invest Ophthalmol Vis Sci 2017;58:5201–5208. [PubMed: 29049720]
15. Qu Y, Gong D, Yu W, Dong F. Characteristics of the Choriocapillaris Layer in Optical Coherence Tomography Angiography of Acute Central Serous Chorioretinopathy. Ophthalmic Surg Lasers Imaging Retina 2017;48:1000–1005. [PubMed: 29253303]

16. Guduru A, Al-Sheikh M, Gupta A, Ali H, Jalali S, Chhablani J. Quantitative Assessment of the Choriocapillaris in Patients With Retinitis Pigmentosa and in Healthy Individuals Using OCT Angiography. Ophthalmic Surg Lasers Imaging Retina 2018;49:e122–e128. [PubMed: 30395672]
17. Yu Y, Teng Y, Gao M, Liu X, Chen J, Liu W. Quantitative Choriocapillaris Perfusion Before and After Vitrectomy in Idiopathic Epiretinal Membrane by Optical Coherence Tomography Angiography. Ophthalmic Surg Lasers Imaging Retina 2017;48:906–915. [PubMed: 29121360]
18. Giannakouras P, Andreanos K, Giavi B, Diagourtas A. Optical Coherence Tomography Angiography: Employing a Novel Technique for Investigation in Vogt-Koyanagi-Harada Disease. Case Rep Ophthalmol 2017;8:362–369. [PubMed: 28868031]
19. Swaminathan SS, Shah P, Zheng F, Gregori G, Rosenfeld PJ. Detection of Choriocapillaris Loss in Alport Syndrome With Swept-Source OCT Angiography. Ophthalmic Surg Lasers Imaging Retina 2018;49:138–141. [PubMed: 29443365]
20. Spaide RF. Choriocapillaris Flow Features Follow a Power Law Distribution: Implications for Characterization and Mechanisms of Disease Progression. Am J Ophthalmol 2016;170:58–67. [PubMed: 27496785]
21. Uji A, Balasubramanian S, Lei J, Baghdasaryan E, Al-Sheikh M, Sadda SR. Choriocapillaris Imaging Using Multiple En Face Optical Coherence Tomography Angiography Image Averaging. JAMA Ophthalmol 2017;135:1197–1204. [PubMed: 28983552]
22. Borrelli E, Shi Y, Uji A, et al. Topographic Analysis of the Choriocapillaris in Intermediate Age-related Macular Degeneration. Am J Ophthalmol 2018;196:34–43. [PubMed: 30118688]
23. Takayama K, Kaneko H, Ito Y, et al. Novel Classification of Early-stage Systemic Hypertensive Changes in Human Retina Based on OCTA Measurement of Choriocapillaris. Sci Rep 2018;8:15163. [PubMed: 30310137]
24. Nesper PL, Soetikno BT, Fawzi AA. Choriocapillaris Nonperfusion is Associated With Poor Visual Acuity in Eyes With Reticular Pseudodrusen. Am J Ophthalmol 2017;174:42–55. [PubMed: 27794427]
25. Sarwar S, Hassan M, Soliman MK, et al. Diurnal variation of choriocapillaris vessel flow density in normal subjects measured using optical coherence tomography angiography. Int J Retina Vitreous 2018;4:37. [PubMed: 30338130]
26. Choi W, Waheed NK, Moult EM, et al. Ultrahigh Speed Swept Source Optical Coherence Tomography Angiography of Retinal and Choriocapillaris Alterations in Diabetic Patients with and without Retinopathy. Retina 2017;37:11–21. [PubMed: 27557084]
27. Thulliez M Correlations Between Choriocapillaris Flow Deficits Around Geographic Atrophy and Enlargement Rates Based on Swept Source OCT Imaging. J Fr Ophtalmol 2018;41:569–570. [PubMed: 29887408]
28. Zhang Q, Zhang A, Lee CS, et al. Projection artifact removal improves visualization and quantitation of macular neovascularization imaged by optical coherence tomography angiography. Ophthalmol Retina 2017;1:124–136. [PubMed: 28584883]
29. Chu Z, Chen CL, Zhang Q, et al. Complex signal-based optical coherence tomography angiography enables in vivo visualization of choriocapillaris in human choroid. J Biomed Opt 2017;22:1–10.
30. Zhang A, Zhang Q, Chen CL, Wang RK. Methods and algorithms for optical coherence tomography-based angiography: a review and comparison. J Biomed Opt 2015;20:100901. [PubMed: 26473588]
31. Zhang A, Zhang Q, Wang RK. Minimizing projection artifacts for accurate presentation of choroidal neovascularization in OCT micro-angiography. Biomed Opt Express 2015;6:4130–43. [PubMed: 26504660]
32. Wang RK, An L, Francis P, Wilson DJ. Depth-resolved imaging of capillary networks in retina and choroid using ultrahigh sensitive optical microangiography. Opt Lett 2010;35:1467–9. [PubMed: 20436605]
33. Zhang Q, Zheng F, Motulsky EH, et al. A Novel Strategy for Quantifying Choriocapillaris Flow Voids Using Swept-Source OCT Angiography. Invest Ophthalmol Vis Sci 2018;59:203–211. [PubMed: 29340648]

34. Chu Z, Zhou H, Cheng Y, Zhang Q, Wang RK. Improving visualization and quantitative assessment of choriocapillaris with swept source OCTA through registration and averaging applicable to clinical systems. Sci Rep 2018;8:16826. [PubMed: 30429502]

35. Kurokawa K, Liu Z, Miller DT. Adaptive optics optical coherence tomography angiography for morphometric analysis of choriocapillaris [Invited]. Biomed Opt Express 2017;8:1803–1822. [PubMed: 28663867]

36. Gorczynska I, Migacz JV, Jonnal R, Zawadzki RJ, Poddar R, Werner JS. Imaging of the human choroid with a 1.7 MHz A-scan rate FDML swept source OCT system: SPIE, 2017:10.

37. Poddar R, Migacz JV, Schwartz DM, Werner JS, Gorczynska I. Challenges and advantages in wide-field optical coherence tomography angiography imaging of the human retinal and choroidal vasculature at 1.7-MHz A-scan rate. J Biomed Opt 2017;22:1–14.

38. Zhang Q, Chen CL, Chu Z, et al. Automated Quantitation of Choroidal Neovascularization: A Comparison Study Between Spectral-Domain and Swept-Source OCT Angiograms. Invest Ophthalmol Vis Sci 2017;58:1506–1513. [PubMed: 28273317]

39. Tokayer J, Jia Y, Dhalla AH, Huang D. Blood flow velocity quantification using split-spectrum amplitude-decorrelation angiography with optical coherence tomography. Biomed Opt Express 2013;4:1909–24. [PubMed: 24156053]

40. Makita S, Jaillon F, Yamanari M, Miura M, Yasuno Y. Comprehensive in vivo micro-vascular imaging of the human eye by dual-beam-scan Doppler optical coherence angiography. Opt Express 2011;19:1271–83. [PubMed: 21263668]

41. Waheed NK, Moult EM, Fujimoto JG, Rosenfeld PJ. Optical Coherence Tomography Angiography of Dry Age-Related Macular Degeneration. Dev Ophthalmol 2016;56:91–100. [PubMed: 27023214]

42. Spaide RF, Curcio CA. Evaluation of Segmentation of the Superficial and Deep Vascular Layers of the Retina by Optical Coherence Tomography Angiography Instruments in Normal Eyes. JAMA Ophthalmol 2017;135:259–262. [PubMed: 28097291]

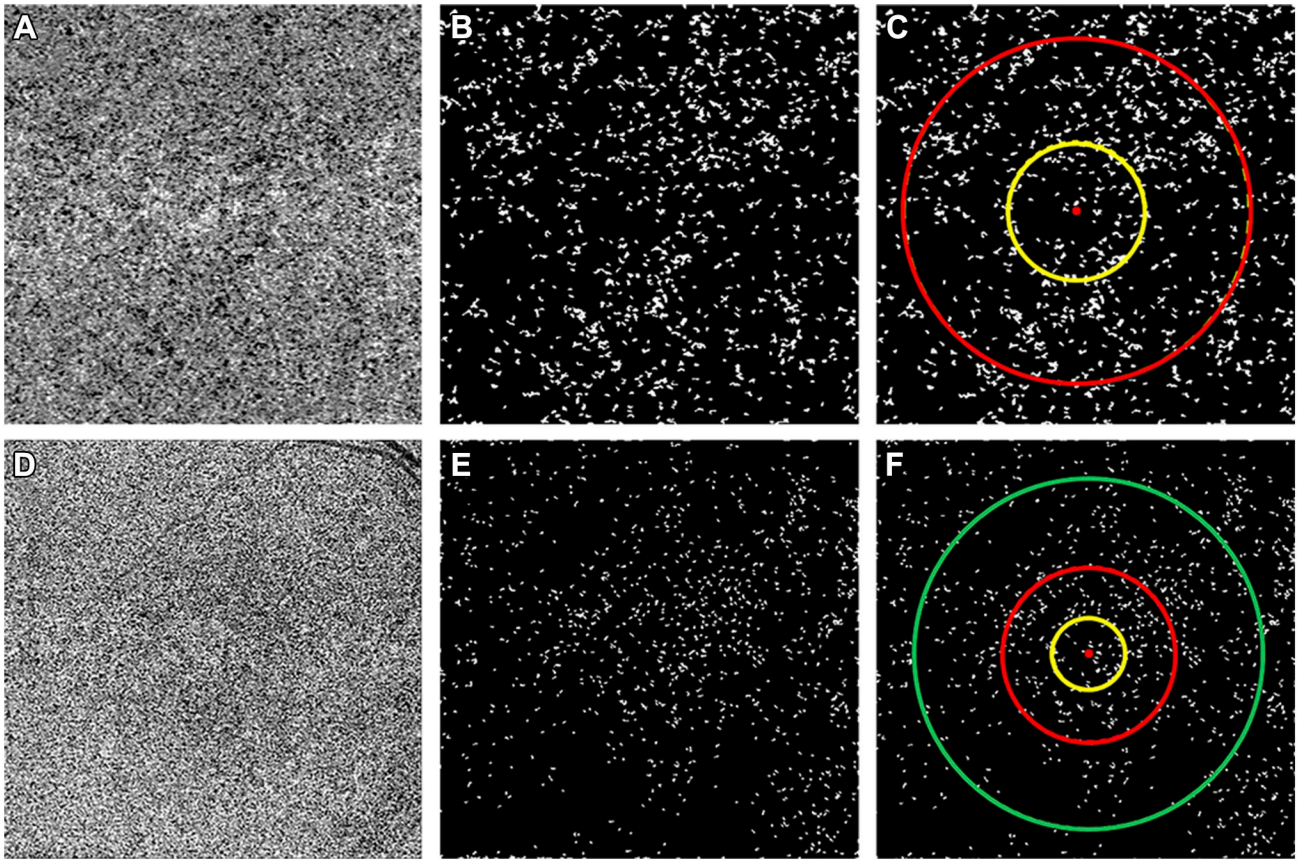

FIGURE 1:

Visualization of the choriocapillaris (CC) and the regions used to calculate the average area of flow deficits (FDa) in 3×3 mm and 6×6 mm scans using SS-OCTA.

(**A**) CC *en face* flow image from a 3×3 mm scan following retinal vessel projection artifact removal and compensation. (**B**) CC binary image used for CC FDa analysis with CC flow deficits represented as white in the 3×3 mm scan. (**C**) Regions used for CC analysis in the 3×3 mm scan with the yellow circle representing the central 1 mm circle centered on the fovea (C_1 region) and red circle representing the central 2.5 mm circle centered on the fovea ($C_{2.5}$ region). (**D**) CC *en face* flow image from a 6×6 mm scan following retinal vessel projection artifact removal and compensation. (**E**) CC binary image used for CC FDa analysis with CC flow deficits represented as white in 6×6 mm scan. (**F**) Regions used for CC analysis in the 6×6 mm scan with the yellow circle representing the central 1 mm circle centered on the fovea (C_1 region), the red circle representing the central 2.5 mm circle centered on the fovea ($C_{2.5}$ region), and the green circle representing the central 5 mm circle centered on the fovea (C_5 region).

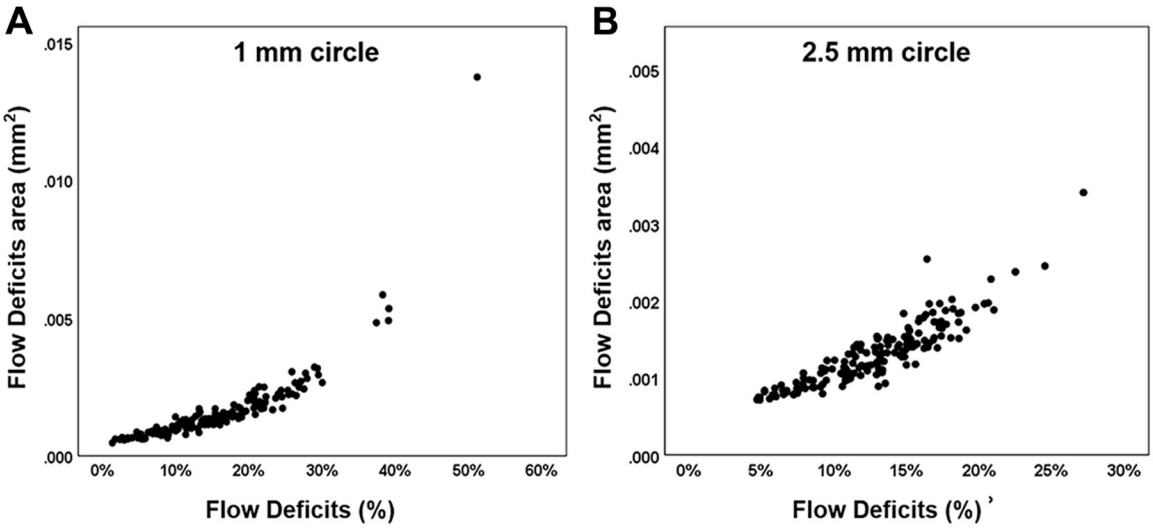

FIGURE 2:

Correlation between the average area of CC flow deficits (FDa) and the percentage of flow deficits (FD%) in the 1mm circles and 2.5 mm circles from the 3×3 mm scans. The average area of flow deficits and the percentage of flow deficits are compared in the 3×3 mm scans for the 1 mm circles (**A**) and 2.5 mm circles (**B**) centered on the fovea. Pearson's r correlations were 0.83 and 0.90 for 1mm and 2.5mm circles, respectively.

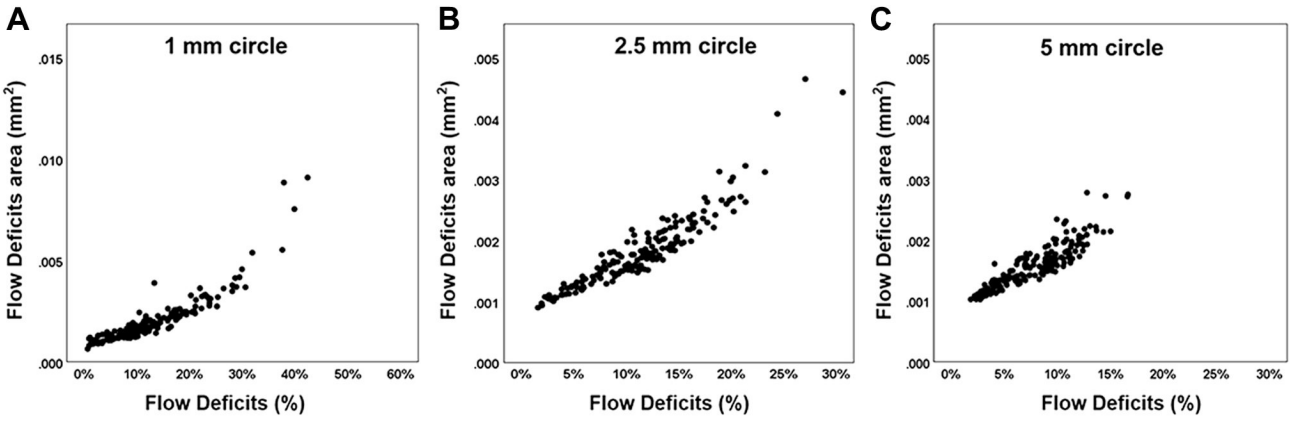

FIGURE 3:

Correlation between the average area of flow deficits (FDa) and the percentage of flow deficits (FD%) in the 1mm circles, 2.5 mm circles, and 5 mm circles from the 6×6 mm scans. The average area of flow deficits and the percentage of flow deficits are compared in the 6×6 mm scans for the 1 mm circles (**A**), 2.5 mm circles (**B**),and 5 mm circles (**C**) centered on the fovea. Pearson's r correlations were 0.90, 0.89, and 0.89 for 1mm, 2.5mm, and 5mm circles, respectively.

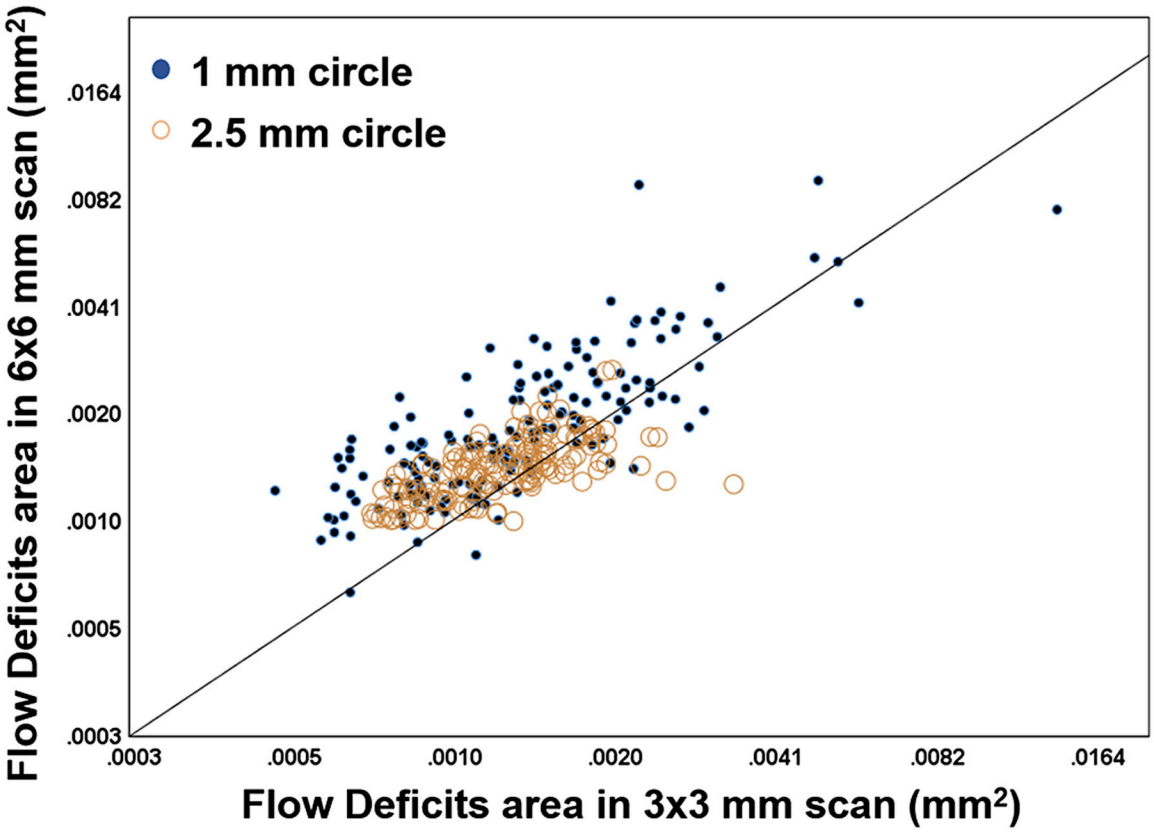

FIGURE 4:

Correlations between the average area of flow deficits (FDa) within the 1 mm circles and 2.5 mm circles from the 3×3 mm scans and the 6×6 mm scans. Pearson's r correlations were 0.72 and 0.56 for the 1 mm and 2.5 mm circles, respectively.

Table 1:

The average area of choriocapillaris flow deficits in the 3×3 mm scans by each decade of age.

	Age Group						
Region	**19–29**	**30–39**	**40–49**	**50–59**	**60–69**	**70–79**	**80–89**
Quantified	**N=18**	**N=23**	**N=22**	**N=23**	**N=28**	**N=31**	**N=19**
1 mm Circle, mm^2 (SD) [range]	0.0008 (0.0003) [0.0005–0.0014]	0.0010 (0.0003) [0.0006–0.0020]	0.0012 (0.0003) [0.0006–0.0018]	0.0015 (0.0004) [0.0008–0.0025]	0.0015 (0.0005) [0.0008–0.0024]	0.0022 (0.0010) [0.0008–0.0049]	0.0028 (0.0029) [0.0010–0.0137]
2.5 mm Circle, mm^2 (SD) [range]	0.0009 (0.0001) [0.0007–0.0013]	0.0010 (0.0002) [0.0007–0.0017]	0.0012 (0.0004) [0.0007–0.0025]	0.0014(0.0002) [0.0010–0.0019]	0.0013(0.0003) [0.0009–0.0020]	0.0016 (0.0004) [0.0008–0.0025]	0.0017(0.0005) [0.0012–0.0034]

Abbreviation: SD= standard deviation

Table 2:

The average area of choriocapillaris flow deficits in the 6×6 mm scans by each decade of age.

Age Group							
Region	**19–29**	**30–39**	**40–49**	**50–59**	**60–69**	**70–79**	**80–89**
Quantified	**N=18**	**N=23**	**N=22**	**N=23**	**N=28**	**N=31**	**N=19**
1 mm Circle, mm^2 (SD) [range]	0.0012 (0.0003) [0.0008–0.0019]	0.0013 (0.0003) [0.0006–0.0018]	0.0015 (0.0005) [0.0009–0.0031]	0.0023 (0.0009) [0.0009–0.0042]	0.0020 (0.0006) [0.0012–0.0032]	0.0027 (0.0016) [0.0010–0.0090]	0.0031 (0.0020) [0.0012–0.0088]
2.5 mm Circle, mm^2 (SD) [range]	0.0013 (0.0003) [0.0009–0.0022]	0.0015 (0.0004) [0.0009–0.0024]	0.0016 (0.0004) [0.0010–0.0027]	0.0021 (0.0007) [0.0011–0.0047]	0.0019 (0.0004) [0.0013–0.0027]	0.0021 (0.0006) [0.0013–0.0044]	0.0023 (0.0006) [0.0016–0.0041]
5 mm Circle, mm^2 (SD) [range]	0.0012 (0.0002) [0.0010–0.0016]	0.0014 (0.0003) [0.0010–0.0021]	0.0015 (0.0002) [0.0010–0.0018]	0.0017 (0.0003) [0.0011–0.0028]	0.0017 (0.0003) [0.0012–0.0028]	0.0018(0.0003) [0.0012–0.0027]	0.0019 (0.0003) [0.0014–0.0023]

Abbreviation: SD= standard deviation